**Figure 5–1.** Illustration of a loudness model based on simulations of basilar membrane and auditory nerve responses. **A.** Simulated activity pattern of a population of ANFs with characteristic frequencies from 40 Hz to 13 kHz in response to brief 1-kHz tones from 0 to 90 dB SPL. The simulations were obtained using a modified version of the MAP model (Meddis et al., 2013). At high sound intensities, the spread of excitation is very pronounced, as the 1-kHz tones also strongly excite ANFs with the highest characteristic frequencies. **B.** Relation between the summed activity of all model ANFs (summed excitation) and the perceived loudness in sones according to ANSI S3.4-2007. The dashed line shows a fitted power-law function with a slope of 1.1, illustrating that perceived loudness is proportional to the overall sound-evoked activity in the auditory nerve.
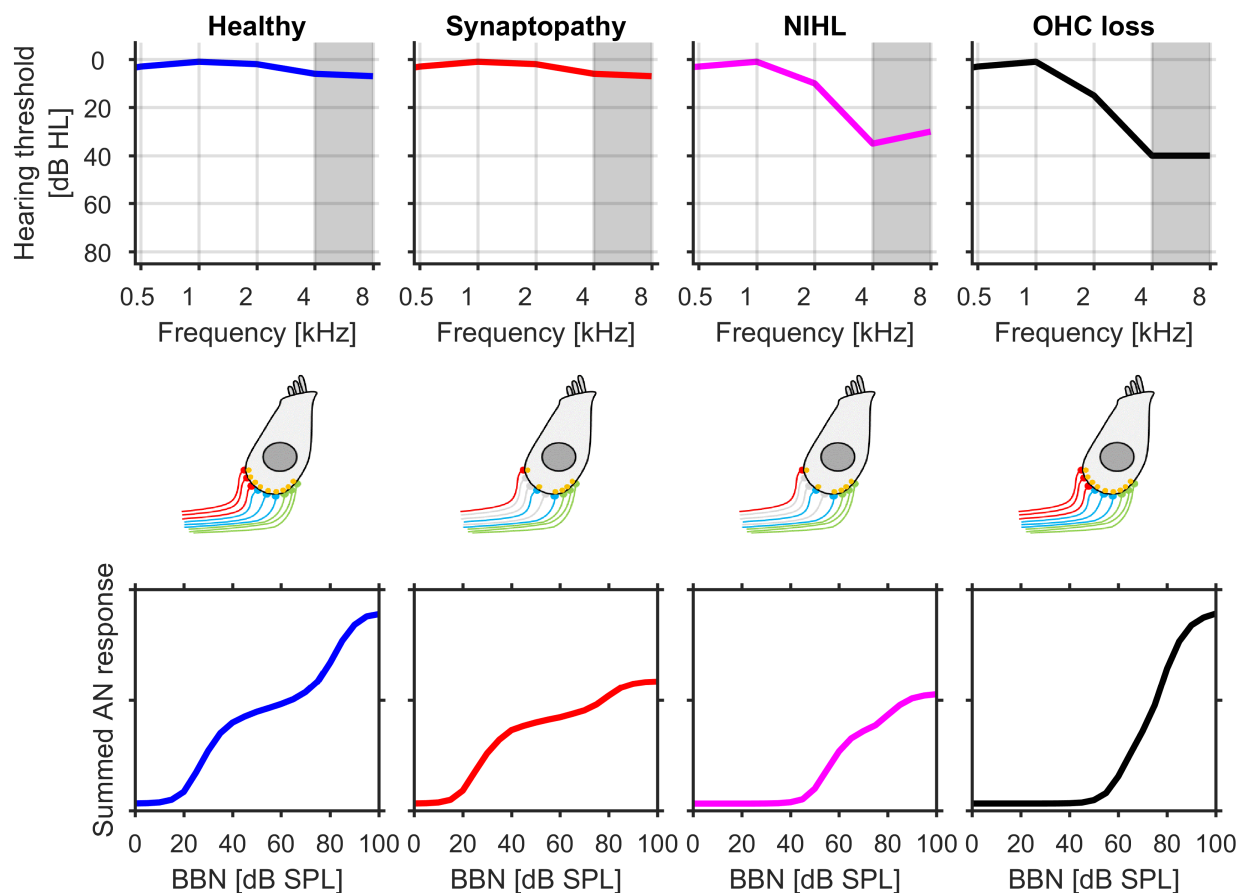
Figure 5–2. Simulation of the effects of different types of damage to or loss of cochlear hair cells on ANF responses. (Top row) Generic audiograms for noise-induced cochlear synaptopathy (hidden hearing loss), noise-induced hearing loss (NIHL), and outer hair cell (OHC) loss. (Middle row) Schematic picture of an IHC with type I ANFs, to illustrate the degree of cochlear synaptopathy, which renders the affected fibers unresponsive to sound (gray fibers). (Bottom row) Simulated AN population responses for AN fibers with characteristic frequencies of 4 to 8 kHz (indicated by shaded area in the top row). The MAP model (Meddis et al., 2013) has been used to simulate AN responses to short bursts of broadband noise for an AN fiber population comprising low-, medium-, and high-threshold AN fibers, with the extent of hearing loss corresponding to the audiograms in the top row. For NIHL, a combination of stereocilia damage, synaptopathy, and hair cell loss was assumed. The simulations demonstrate that the different kinds of damage to cochlear hair cells all reduce overall AN responses, indicating that damage to cochlear hair cells is unlikely to produce a neural correlate of loudness hyperacusis at the level of the AN.
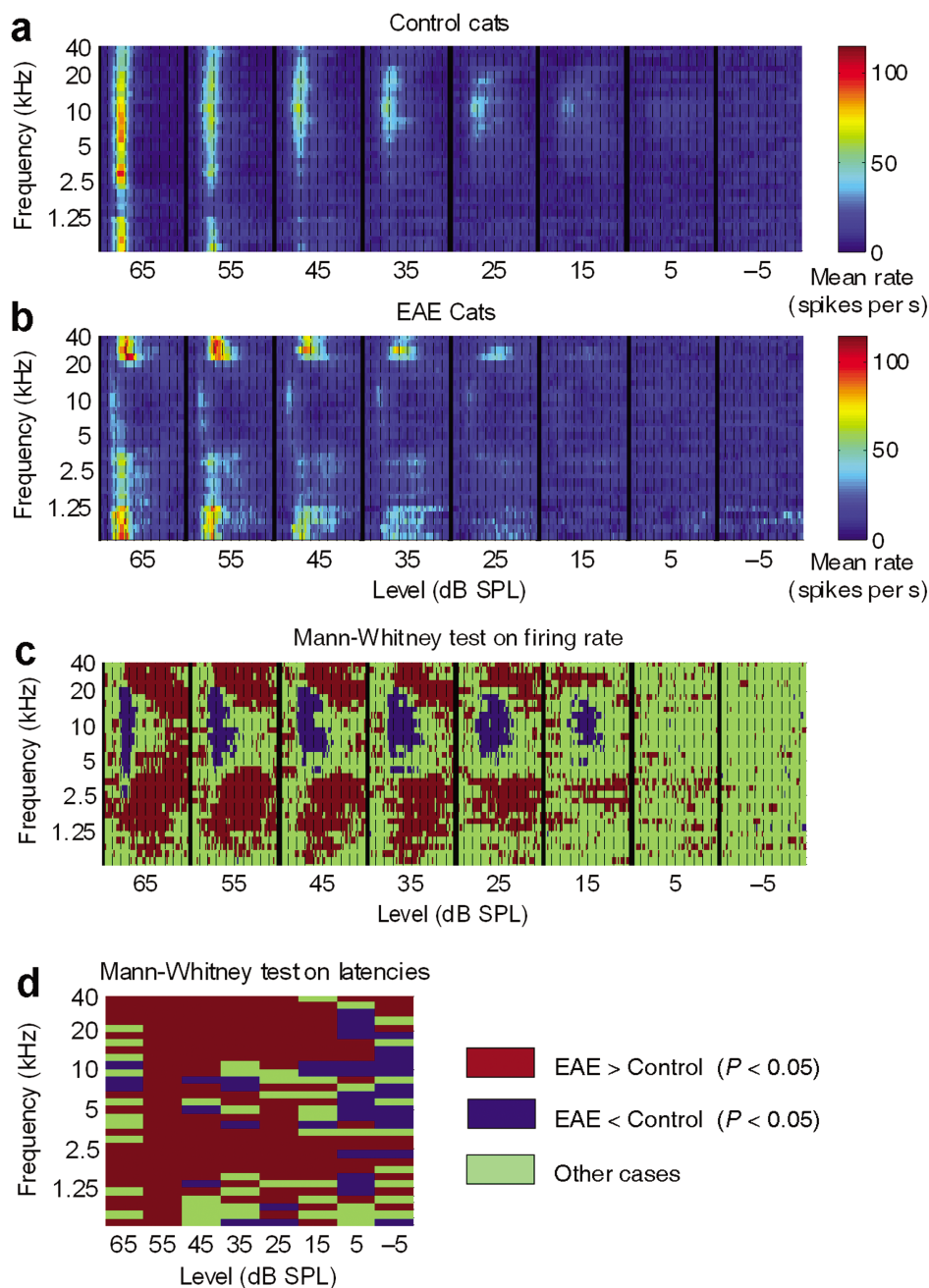
Figure 8–1. Averaged poststimulus time histograms across all control and EAE cats. (**a, b**) Averaged PSTHs (2-ms time bins) as a function of SPL, over a 100-ms time window, in control and EAE cats. Dashed lines, 10-ms intervals. Colored bars, mean firing rate. In control cats, the mean response suggested that the highest sensitivity (lowest thresholds) was to frequencies around 10 kHz and that the largest responses were to frequencies between 2.5 kHz and 10 kHz. In EAE cats, the most sensitive frequencies were those below 1.25 kHz and above 20 kHz. Note that neural responses in EAE cats were much more spread out over time compared to those in control cats. (**c, d**) Graphical representation of significant differences (Mann-Whitney test) between EAE and control groups in terms of (**c**) mean firing rate per frequency-latency bin and (**d**) mean latency per frequency-intensity bin. *Source*: From Noreña et al. (2006).
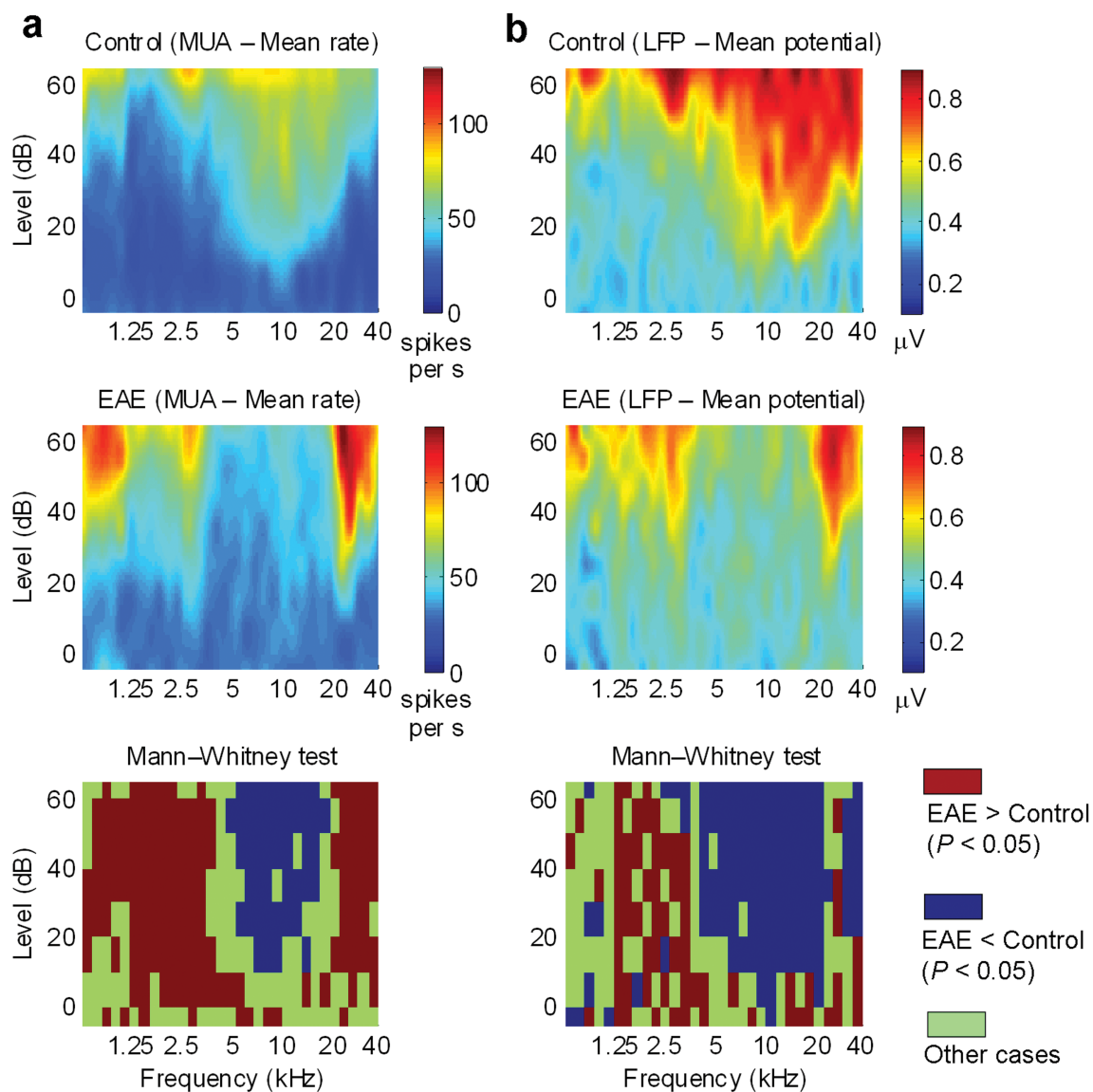
Figure 8–2. Averaged group multiunit firing rates and LFP amplitude as a function of frequency and intensity. First row, averaged multiunit firing rate; second row, averaged LFP amplitude; third row, results of statistical tests (Mann-Whitney) for comparisons between control and EAE cats. *Source*: From Noreña et al. (2006).
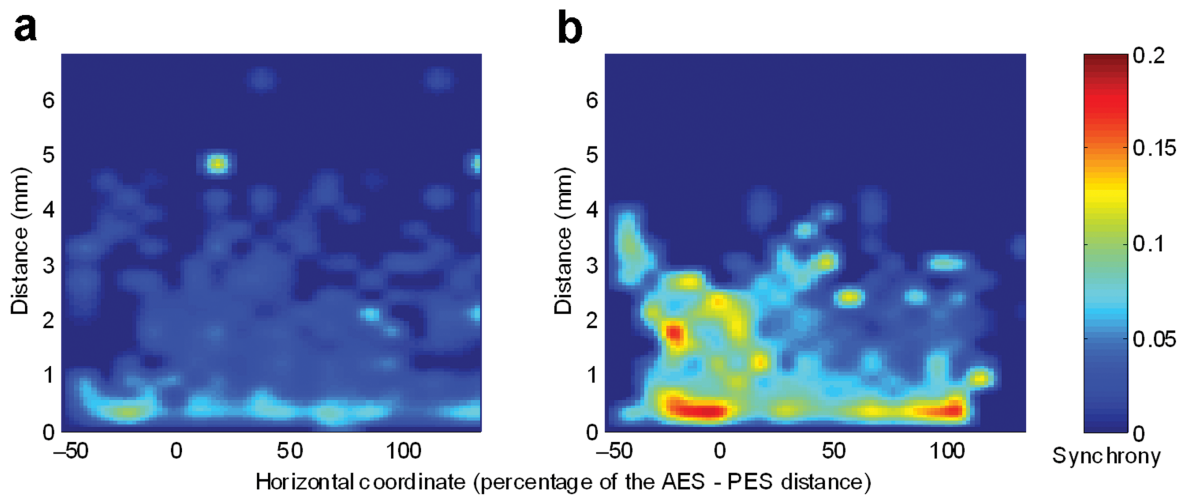
Figure 8–3. Neural synchrony maps in primary auditory cortex. (**a, b**) Synchrony, defined here as the peak strength of the corrected cross-correlogram (Methods), as a function of the position of the recording electrode along the postero-anterior axis (abscissa) and the distance between the two electrodes involved in the calculation of synchrony (ordinate), in (**a**) control and (**b**) EAE cats. For each electrode pair, positions along the postero-anterior axis are plotted. Bar colors reflect strength of neural synchrony. In control cats, the strongest synchrony was found between neighboring electrodes in the array and most correlations occurred locally. Note the increased synchrony in EAE cats compared to control cats, especially for larger distances between electrodes. This probably signifies the stronger connections over large distances (that is, into the reorganized region) made by horizontal fibers. In these cats, the range of strong correlations is much larger, especially in the −50% to +50% region, which reflects the entire area with characteristic frequencies <4 kHz but also a substantial part of the 5 to 20 kHz area. In addition, the area with characteristic frequencies above 20 kHz (70 to 125%) also showed strongly increased neural synchrony. It is noted that SFR was significantly increased in the region with putative CFs <4 kHz as well as the region with CFs >20 kHz. No significant change was found in the 5 to 20 kHz area. *Source*: From Noreña et al. (2006).
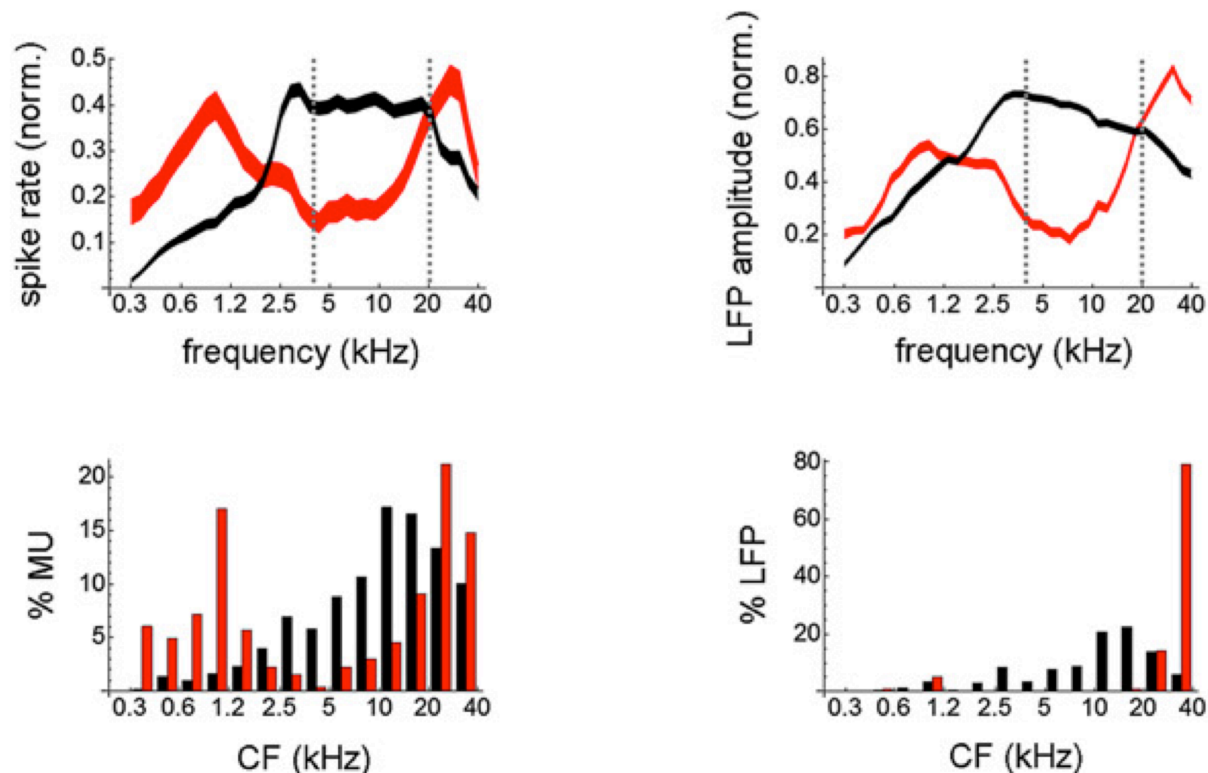
Figure 8–4. Population frequency tuning in A1, pooled across four individual noise-exposed (4 to 20 kHz steeply filtered noise, 68 dB SPL for 6 weeks) and control cats. Top row: averaged frequency marginals from control (black) and noise-exposed (red) cats. Curve thickness illustrates the Bonferroni-corrected 95% confidence interval for the mean, dotted lines mark the 4 to 20 kHz noise bandwidth. Left column based on MU activity, right column based on LFP amplitude. Bottom row: histogram distributions of response characteristic frequencies (CFs of frequency-tuning curves) or best frequencies (BFs of spectro-temporal receptive fields, STRFs) from control (black) and noise-exposed (red) cats (half-octave bin width). *Source*: Reprinted with permission from Pienkowski et al. (2011).